Fabrication and characterization of multiband solar cells based on highly mismatched alloys

N López[1], A F Braña[1], C García Núñez[1], M J Hernández[1], M Cervera[1], M Martínez[1], K M Yu[2,3], W Walukiewicz[3], B J García[1]

[1]Grupo de Electrónica y Semiconductores, Departamento de Física Aplicada, Universidad Autónoma de Madrid, Spain.
[2]Department of Physics and Materials Science, City University of Hong Kong, China.
[3]Materials Sciences Division, Lawrence Berkeley National Laboratory, 1 Cyclotron Road, Berkeley, California 94720, USA.

E-mail: nair.lopez@uam.es

Abstract Multiband solar cells are one type of third generation photovoltaic devices in which an increase of the power conversion efficiency is achieved through the absorption of low energy photons while preserving a large band gap that determines the open circuit voltage. The ability to absorb photons from different parts of the solar spectrum originates from the presence of an intermediate energy band located within the band gap of the material. This intermediate band, acting as a stepping stone allows the absorption of low energy photons to transfer electrons from the valence band to the conduction band by a sequential two photons absorption process. It has been demonstrated that highly mismatched alloys offer a potential to be used as a model material system for practical realization of multiband solar cells. Dilute nitride $GaAs_{1-x}N_x$ highly mismatched alloy with low mole fraction of N is a prototypical multiband semiconductor with a well-defined intermediate band. Currently, we are using chemical beam epitaxy to synthesize dilute nitride highly mismatched alloys. The materials are characterized by a variety of structural and optical methods to optimize their properties for multiband photovoltaic devices.

1. Introduction

Recent attempts to increase the efficiency of solar cells beyond the Shockley and Queisser limit [1] have resulted in many novel device concepts. Among these the multiband solar cells (MSC) concept has been suggested and widely investigated [2,3]. The high power conversion efficiency of MSC arises from the increased photocurrent through absorption of low energy photons by the intermediate band (IB) while preserving a large band gap that determines the open circuit voltage. Several approaches have been proposed to implement the MSC device structure [2-4]. The existence of an IB has been demonstrated in a new class of alloys-highly mismatched alloys (HMAs) [5]. For example, substituting small amount of N atoms in GaAs splits the conduction band (E_C) of GaAs into two sub-bands: a low energy E_- and a higher energy E_+ bands [6-8]. The E_- band plays the role of the IB while the E_+ band becomes the E_C of the $GaAs_{1-x}N_x$ alloy.

The current work presents our study on the IB materials grown using a chemical beam epitaxy (CBE) system. The presence of an IB and the detection of the E_+ to E_- transition were studied using

photoluminescence (PL) and photoreflectance (PR) techniques. The materials are characterized by a variety of structural and optical methods to optimize their performance for multiband photovoltaic devices. Additionally, the experimental results are analyzed with the band anticrossing model (BAC) showing an excellent agreement between experimental results and theoretical model.

2. Experimental

A CBE system has been used to grow the multiband HMA thin films under ultra-high vacuum conditions using gas precursors, which are in liquid phase at room temperature in equilibrium with their subatmospheric vapor pressure. The structure of the MSC consists of a p/n junction of the HMA layers sandwiched between a p or n blocking layers [10]. These blocking layers isolate the IB from the ohmic contacts so as to avoid the charge transport from the IB to the contacts. Therefore under solar irradiation three quasi-Fermi levels associated with the three bands of the material will form. This condition is necessary in order to preserve the open circuit voltage determined by the largest band gap of the material (E_+-E_V) [10]. Figure 1 shows a schematic of a MSC structure (inset) and its corresponding band diagram.
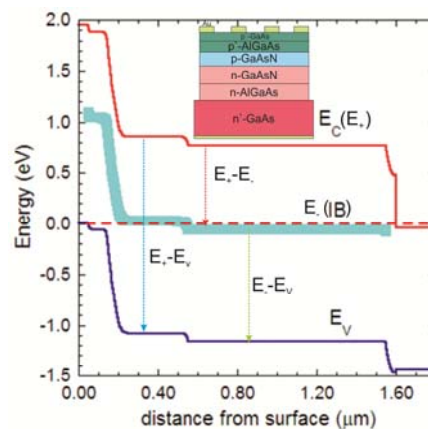

Figure 1. Structure and band diagram of a blocked intermediate band solar cell. The sub-band gap transitions from E_C (E_+) to the IB (E_-) are denoted as E_+-E_-, from E_- to E_V as E_--E_V and finally from E_+ to valence band (E_V) as E_+-E_V.

Dimethylhydrazine (DMHy), triethylgalium (TEGa) and tertiarybutylarsine (TBAs) precursors were used to grow $GaAs_{1-x}N_x$ layers by CBE. The gas precursor control system enables the control of fluxes of individual species on the substrate surface.

Fluxes of the different precursors determine both the growth rate as well as the alloy composition, which in turn determines the locations of the various band edges [11]. An alloy with an N mole fraction in the range $x_N=0.02$ to $x_N=0.03$ has the optimum band gap energies for an IB device [12]. To form a p/n junction Trimethyltin (TMSn) was used for n-type and carbon tetrabromide (CBr4) for p-type doping. Dopant levels have been chosen to optimize the performance of the device.

$Al_xGa_{1-x}As$ alloys were inserted as blocking layers during growth using tritertiary-bultylaluminum (TTBAl) as precursor for Al. This precursor is able to introduce high Al mole fractions [13]with a residual p-type doping level in the 10^{17} cm^{-3} range allowing to form $Al_xGa_{1-x}As$ layers with up $x_{Al} = 0.45$. A very thin p-GaAs capping layer was grown on the top of the structure to avoid oxidation of the $Al_xGa_{1-x}As$ layer.

3. Results

To obtain materials with the optimal band structure for a multiband device, growth parameters including substrate temperature, growth rate, fluxes of the various gas precursors were varied. N concentration of the samples was determined by measuring energies of interband transitions by PR and PL techniques. To obtain $GaAs_{1-x}N_x$ alloy with a band gap of close to 2 eV the N mole fraction should

be $x_N=0.023$. For this composition the IB(E_-) is located at 1.17 eV above the E_V and 0.86 eV below E_+. The growth parameters were fixed at a growth rate of 0.5 μm/h, substrate temperature of 500 ℃ and a DMHy flux of 3 Torr. The energies of the E_+ and E_- are given by the BAC model (equation 1 [6, 7]).

$$E_\pm = \frac{(E_N + E_M) \pm \left[(E_N - E_M)^2 + 4V_{NM}^2 x\right]^{1/2}}{2} \qquad (1)$$

where E_N is the energy of localized N level, E_M is the conduction band edge of the GaAs matrix and $V_{NM}=2.7$ eV is the coupling constant [6]. The $E_-(k=0)$ and $E_+(k=0)$ represents the intermediate and the conduction band edge, respectively. The E_V edge is not affected by the BAC and experiences only small downward shift of 20 meV per % of N content due to the E_V offset of GaAs and GaN. Figure 2 (a) shows the measured N mole fraction in GaAs$_{1-x}$N$_x$ layers as a function of the DMHy flux.

In order to calibrate the growth of Al$_x$Ga$_{1-x}$As blocking layers, Al$_x$Ga$_{1-x}$As layers were grown with a growth rate of 0.3 μm/h at a substrate temperature of 560 ℃ using different TTBAl fluxes; the composition of the grown layers was determined using spectroscopic ellipsometry (SE), PL and PR techniques. Figure 2 (b) shows the obtained dependence of the incorporated Al mole fraction as a function of the TTBAl flux used for different samples.
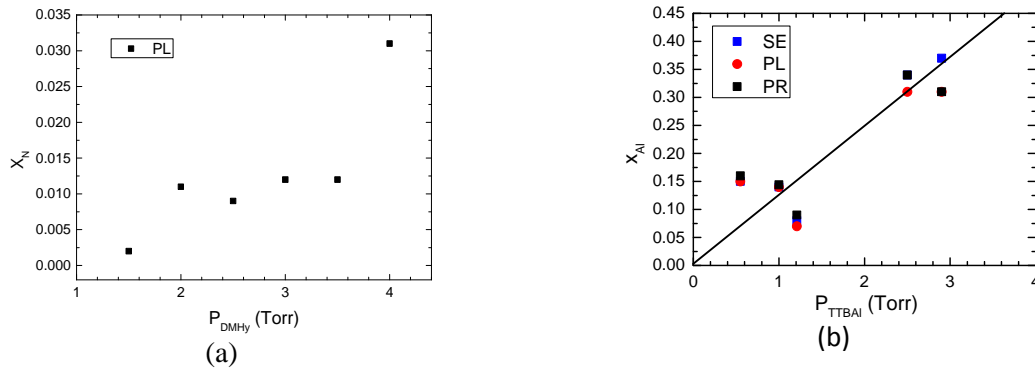

(a)   (b)

Figure 2. (a) N mole fraction in GaAs$_{1-x}$N$_x$ as a function of DMHy gas precursor flux at a growth rate of 0.5 μm/h and a substrate temperature of 500 ℃. (b) Al mole fraction in Al$_x$Ga$_{1-x}$As as a function of TTBAl gas precursor flux at a growth rate of 0.3μm/h and a substrate temperature of 560 ℃.

Finally, using the growth parameters determined from the calibration runs two blocked intermediate band (BIB) solar cells have been grown with different N content by varying the DMHy flux. In the dilute GaA$_{1-x}$N$_x$ alloy, the interaction between the localized N states and the extended states of the E_C of host GaAs matrix splits the E_C into two subbands. PL measurements on these samples demonstrated the presence of an IB(E_-) in both samples. As it is presented in Figure 3 (a) both transitions involving the IB are clearly observed for the sample grown with 3.75 Torr of DMHy. The low energy emission at 0.97 eV corresponds to the transitions between E_- and E_V whereas the higher energy peak at 1.21 eV can be attributed to the transition from E_+ to E_-; from this spectrum we observe that the E_- band is closer in energy to the E_V than to the $E_C(E_+)$. The N mole fraction for this sample is about $x_N=0.05$ which is significantly higher than the concentration of about $x_N=0.03$ estimated from the calibration samples. In addition, the PL spectrum shows a third peak at 1.37 eV which probably corresponds to a transition between E_- (IB) and the E_V of the AlGaAs blocking layer.

The PL spectra were analyzed using the BAC model. Figure 3 (b) shows the band gaps of GaAs$_{1-x}$N$_x$ as a function of the N mole fraction as calculated by the BAC model at low temperatures (12 K). The solid blue line corresponds to E_+ also denoted as the E_C of the GaAs$_{1-x}$N$_x$ alloy. The green line represents the energy level E_- that is equal to the energy separation $E_- - E_V$. Finally, the solid red line is the energy separation between $E_+ - E_-$. The green-dash line and red-dash line are the PL energies measured for the sample grown with 3.75 Torr of DMHy pressure flux (red spectrum in figure 3a). Both PL transitions are in an excellent agreement with the transition energies predicted for a sample with $x_N=0.05$. Table 1 presents the theoretical calculation for the sub-band gaps and the PL experimental values. Also, as is observed in PL measurements, the E_- band is located closer to the E_V

than the conduction band (E_+). The BAC calculations show that the two sub-band gaps intersect for N content of about $x_N=0.04$.

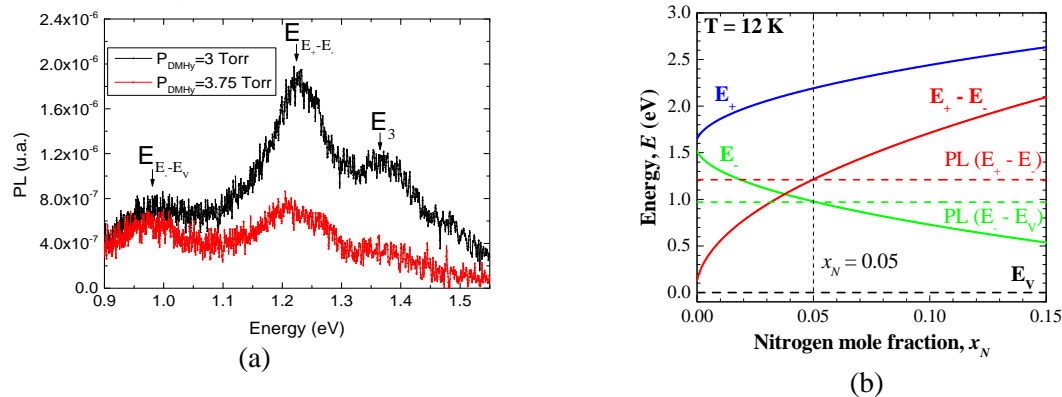(a)   (b)

Figure 3. (a) Low temperature (12 K) photoluminescence measurements of samples grown with 3 Torr (black spectrum) and 3.75 Torr (red spectrum) of DMHy flux. (b) Theoretical calculations of the low temperature (12 K) sub-band gaps versus the N concentration using the BAC model are represented with solid lines. Dash lines correspond with the PL energy values.

Table 1. Theoretical and experimental values of the sub-band gaps for a sample with x = 0.05 of N.

	E_+-E_- (eV)	E_--E_V (eV)
BAC calculation	1.214	0.977
PL measurement	1.21	0.97

4. Conclusions

A chemical beam epitaxy system has been used to grow multiband solar cells based on a p/n junction of $GaAs_{1-x}N_x$ sandwiched between p and n blocking layers of $Al_xGa_{1-x}As$. The growth of $GaAs_{1-x}N_x$ and $Al_xGa_{1-x}As$ layers was optimized at 500 ºC (0.5 μm/h) and 560 ºC (0.3 μm/h) respectively. Two full structures have been grown with different N content in the $GaAs_{1-x}N_x$ layers by changing the DMHy flux used. These structures were characterized by PL measurements and studied by the BAC model. PL measurements have shown two emission peaks originating from transitions involving the IB, from E_+ to E_- and from E_- to E_V. The observed transition from E_+ to E_- demonstrates a significant optical coupling between those two bands. Comparison of the BAC model calculations with the experimental results allows for the determination of N concentration in the cell structures.

Reference

[1]   W. Shockley and H. J. Queisser, *J. of Appl. Phys.* **32** (1961), 510-519.
[2]   M. Wolf, *Proc. IRE* **48** (1960), 1246.
[3]   A. Luque, et al., *Phys. Rev. Lett.* **78** (1997), 5014.
[4]   N. López, et al., *J. of Solar Energy Engineering ASME* **129** (2007), 319-322.
[5]   N. López, et al., *Phys. Rev. Lett.* **106** (2011), 028701.
[6]   W. Shan, et al., *Phys. Rev. Lett.* **82** (1999), 1221.
[7]   W. Walukiewicz, et al., *Phys. Rev. Lett.* **85** (2000), 1552.
[8]   K. M. Yu, et al., *Phys. Rev. Lett.* **91** (2003), 246403.
[9]   A. Luque et al., *Appl. Phys. Lett.* **87** (2005), 083505.
[10] N. López, et al., *26th EUPVSEC*-1BO.9.4 (2011), 97-100, 3-936338-27-2.
[11] K. M. Yu, et al., *J. Appl. Phys.* **106** (2009), 103709.
[12] L. Cuadra, et al., *IEEE Transactions on Electron Devices* **51** (2004), 1002-1007.
[13] A. Braña, et al., *18th European Molecular Beam Epitaxy Workshop*–TuP.13 (2015), 226.